

Direct Measurement of A_b using Charged Kaons at the SLD Detector*

The SLD Collaboration**

Stanford Linear Accelerator Center

Stanford University, Stanford, CA 94309

Contact: Thomas Wright, twright@slac.stanford.edu

Abstract

We report a new measurement of A_b using data obtained by SLD in 1997-98. This measurement uses a vertex tag technique, where the selection of a b hemisphere is based on the reconstructed mass of the bottom hadron decay vertex. The method uses the 3D vertexing capabilities of SLD's CCD vertex detector and the small and stable SLC beams to obtain a high b -event tagging efficiency and purity of 78% and 97%, respectively. Charged kaons identified by the CRID detector provide an efficient quark-antiquark tag, with the analyzing power calibrated from the data. We obtain a preliminary result of $A_b = 0.997 \pm 0.044 \pm 0.067$

Contributed to the International Europhysics Conference on High Energy Physics, July 15-21 1999, Tampere, Finland; Ref 6-473, and to the XIXth International Symposium on Lepton Photon Interactions, August 9-14 1999, Stanford, USA.

*Work supported by Department of Energy contract DE-AC03-76SF00515 (SLAC).

1 Introduction

Measurements of fermion asymmetries at the Z^0 resonance probe a combination of the vector and axial vector couplings of the Z^0 to fermions, $A_f = 2v_f a_f / (v_f^2 + a_f^2)$. The parameters A_f express the extent of parity violation at the Zff vertex and provide sensitive tests of the Standard Model.

The Born-level differential cross section for the reaction $e^+e^- \rightarrow Z^0 \rightarrow f\bar{f}$ is

$$\frac{d\sigma_f}{dz} \propto (1 - A_e P_e)(1 + z^2) + 2A_f(A_e - P_e)z, \quad (1)$$

where P_e is the longitudinal polarization of the electron beam ($P_e > 0$ for right-handed (R) polarization) and $z = \cos \theta$ is the direction of the outgoing fermion relative to the incident electron. The parameter A_f can be isolated by forming the left-right forward-backward asymmetry $\tilde{A}_{FB}^f(z) = |P_e| A_f 2z / (1 + z^2)$, although in this analysis we work directly with the basic cross section.

This note describes the analysis of the data taken during 1997-98 with the newer VXD3 vertex detector. Analysis of the 1993-95 data taken with the original VXD2 vertex detector is described in [1].

2 The SLD Detector

The operation of the SLAC Linear Collider with a polarized electron beam has been described in detail elsewhere [2]. In 1997-98 a sample of 350k events with average polarization of $|P_e| = 0.733 \pm 0.008$ was collected.

Charged particle tracking and momentum analysis are provided by the Central Drift Chamber [4] and the CCD-based vertex detector [5]. The Liquid Argon Calorimeter (LAC) [6] measures the energy of charged and neutral particles and is also used for electron identification. Muon tracking is provided by the Warm Iron Calorimeter (WIC) [7]. The Cherenkov Ring Imaging Detector (CRID) [8] information (limited to the barrel region) provides particle identification. It consists of liquid and gas Cherenkov radiators illuminating large area UV photon detectors. The combination of the two radiators provides good coverage of the interesting momentum region.

3 Event Selection

Hadronic events are selected based on the visible energy and track multiplicity in the event. The visible energy is measured using central drift chamber (CDC) tracks and must exceed 18 GeV. There must be at least 7 CDC tracks, 3 with hits in the vertex detector. We also require that the thrust axis, measured from calorimeter clusters, satisfy $|\cos\theta_{thr}| < 0.7$. This ensures that the event is contained within the acceptance of the vertex detector. All detector elements are also required to be fully operational. Additionally, we restrict events to 3 jets or less to make sure that we have well defined hemispheres. Jets are defined by the JADE algorithm [9] with $y_{cut} = 0.02$. A total of 250k events pass the above hadronic event selection and jet cut. Background, predominately due to taus, is estimated at $< 0.1\%$.

The SLC interaction point (IP) has a size of approximately $(1.5 \times 0.5 \times 700) \mu\text{m}$ in (x, y, z) . The motion of the IP xy position over a short time interval is estimated to be $\sim 6 \mu\text{m}$. Because this motion is smaller than the xy resolution obtained by fitting tracks to find the primary vertex (PV) in a given event, we use the average IP position for the x and y coordinates of the primary vertex. This average is obtained from tracks with hits in the vertex detector in 30 sequential hadronic events. The z coordinate of the PV is determined event-by-event. This results in a PV uncertainty of $\sim 6 \mu\text{m}$ transverse and $\sim 25 \mu\text{m}$ longitudinal to the beam direction.

3.1 Track Selection

Reconstruction of the mass of heavy hadrons is initiated by identifying secondary vertices in each hemisphere. Only tracks that are well measured are included in the vertex and mass reconstruction. Tracks are required to have at least 23 CDC hits and start within a radius of 50 cm of the IP. The CDC track is also required to extrapolate to within 1.0 cm of the IP in xy and within 1.5 cm of the PV in z . At least two vertex detector hits are required, the combined drift chamber + vertex detector fit must satisfy $\chi^2/d.o.f. < 8$, and $|\cos\theta| < 0.87$. Tracks with an xy impact parameter > 3.0 mm or an xy impact parameter error $> 250 \mu\text{m}$ with respect to the IP are removed from consideration in the vertex reconstruction.

3.2 Vertex Mass Reconstruction

Vertex identification is done topologically. [10]. This method searches for space points in 3D where track density functions overlap. Each track is parameterized by a Gaussian probability density tube with a width equal to the uncertainty in the measured track position at the IP. Points in space where there is a large overlap of probability density are considered as possible vertex points. Final selection of vertices is done by clustering maxima in the overlap density distribution into vertices for separate hemispheres. We found secondary vertices in 86% of bottom, 45% of charm, and 2% of light quark events.

The mass of the secondary vertex is calculated using the tracks that are associated with the vertex. Each track is assigned the mass of a charged pion and the invariant mass of the vertex is calculated. The reconstructed mass is corrected to account for neutral particles as follows. Using kinematic information from the vertex flight path and the momentum sum of the tracks associated with the secondary vertex, we add a minimum amount of missing momentum to the invariant mass. This is done by assuming the true quark momentum is aligned with the flight direction of the vertex. The so-called P_t -corrected mass is given by:

$$M_{VTX} = \sqrt{M_{tk}^2 + P_t^2} + |P_t|$$

where M_{tk} is the mass for the tracks associated with the secondary vertex. We restrict the contribution to the invariant mass that the additional transverse momentum adds to be less than the initial mass of the secondary vertex. This cut ensures that poorly measured vertices in uds events do not leak into the sample by adding large P_t .

3.3 Flavor Tag

We define two tags. A heavy tag is defined as a hemisphere with an invariant mass above $2 \text{ GeV}/c^2$. Requiring at least one of these will ensure high b -purity. The intermediate mass region, between 0.5 and $2 \text{ GeV}/c^2$ contains a mixture of b and c , with a small uds background. The b part of this region is largely B 's which decay so quickly that the track(s) from the W are lost, so only the D tracks are left. Because the cascade K that will be used is among these tracks these vertices are useful, and we define a light tag to be any hemisphere with a vertex, which doesn't pass the heavy tag cuts.

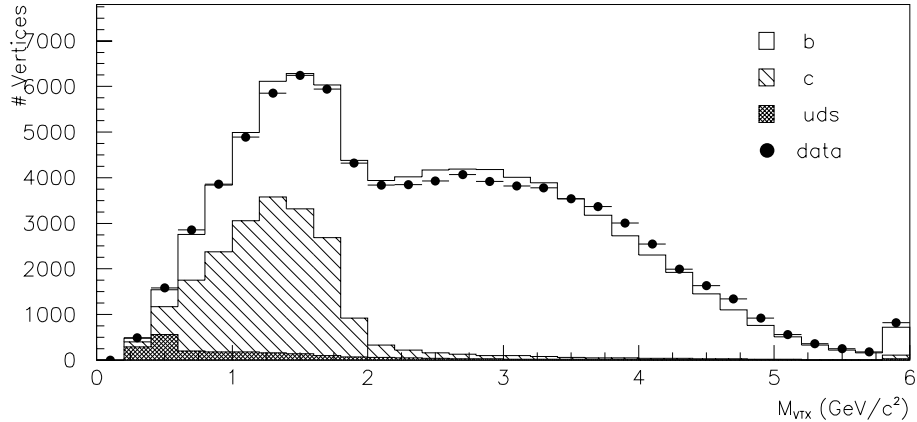


Figure 1: Distribution of M_{VTX} for data (points) and Monte Carlo (solid). The hatched regions represent the light-flavor backgrounds.

These tags are calibrated against the data as described in [11]. The efficiencies η_b (for the light tag) and ϵ_b (for the heavy tag), and partial widths R_b and R_c are found by comparing

the single- vs. double-tagged event rates for the two tags. In addition, the c light tag efficiency η_c can be found from the fraction of events with a light tag in one hemisphere and a heavy tag in the other (mixed tag). The light-flavor efficiencies and ϵ_c are taken from Monte Carlo.

A bottom event is defined to be one with at least one heavy-tagged hemisphere. This is found to be $\sim 78\%$ efficient for bottom events. With the calibrated efficiencies and partial widths the bottom purity of these events is calculated to be $f_c = 96.6 \pm 0.1\%$. This is in good agreement with the Monte Carlo value 96.8% . The c background fraction is 2.6% with uds making up the remainder.

3.4 Signal Tag

The determination of the direction of the quark is done using the kaon charge, Q_K . This is the total charge of the CRID-identified kaon tracks in the vertex. Because of the cascade nature of the tag the signals for $b \rightarrow c \rightarrow s$ and $c \rightarrow s$ decays have the same sign. This reduces sensitivity to the c background fraction.

We see $\sim 25\%$ efficiency for the kaon tag for both charm and bottom events. A hemisphere with two oppositely-charged K tracks is considered uncharged.

The probability to correctly discriminate between quark/antiquark for this tag can be calibrated from the data. The sample used is the events with both hemispheres b -tagged (at least one heavy) and with nonzero charge in each hemisphere. The fraction of these events that are in agreement (opposite charges) can be written as $r_{agree} = p_{correct}^2 + (1 - p_{correct})^2$. This simply says the hemispheres must either be both right or both wrong. After making a correction for the c contamination we find $p_b^{correct} = 70.7 \pm 1.4\%$. The Monte Carlo gives 72.4% . The charm background analyzing power is taken from Monte Carlo, we find $p_c^{correct} = 84.6\%$. Because this procedure calibrates the quark/antiquark flavor at production the B -mixing dilution is automatically included in $p_b^{correct}$.

4 Results

A maximum likelihood fit of all tagged events is used to determine A_b . As a likelihood function we use the total cross section:

$$\mathcal{L} \propto (1 + z^2)(1 - A_e P_e) + 2z(A_e - P_e) [f_b(2p_b^{correct} - 1)A_b + f_c(2p_c^{correct} - 1)A_c] \quad (2)$$

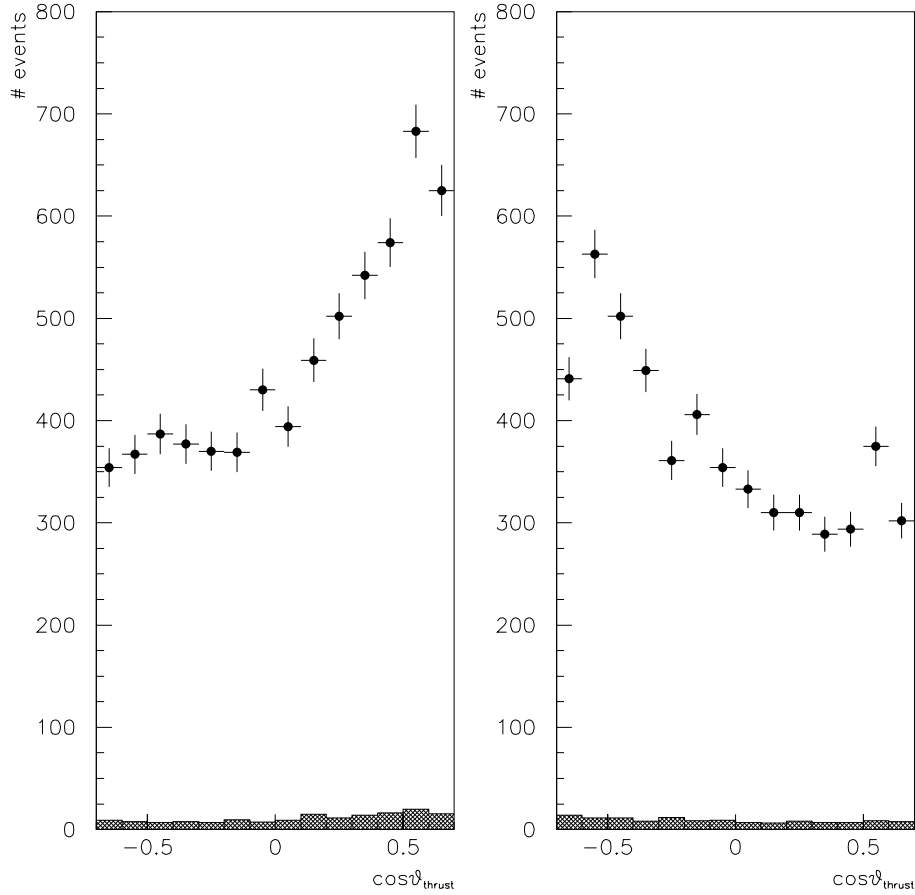


Figure 2: Measured asymmetry for kaon charge. Left side is for left-polarized electrons and right side for right-polarized ones. The hatched region indicates the non- b background.

where $z = -Q \cos \theta_{thr}$, the thrust axis signed by the tagging method described earlier, is an estimate of the quark direction, $f_{b,c}$ is the probability for an event to be b or c respectively, and the factor $(2p^{correct} - 1)$ is the effectiveness of the quark/antiquark tag. The shape of these functions in z is taken from Monte Carlo with the overall normalizations determined from the data. The three signs governing the left-right forward-backward asymmetry – beam polarization P_e , hemisphere tag charge Q , and quark direction $\cos \theta_{thr}$ – are incorporated automatically into the likelihood function.

The QCD corrections to the cross-section are well known [12]. We account for them with a correction term:

$$A_{FB|O(\alpha_s)}^q(\theta) = A_{FB|O(0)}^q(\theta)(1 - \Delta_{O(\alpha_s)}^q(\theta))$$

These QCD corrections have to be adjusted for any bias in the analysis method against $q\bar{q}g$ events:

$$\Delta_{\text{QCD}}^{eff} = f\Delta_{\text{QCD}}$$

Table 1: Systematic errors for the maximum likelihood analysis

Source	δA_b
Tag Composition	
f_b, f_c	0.001
Analyzing Power	
$p_b^{correct}$	0.063
Tracking efficiency 3%	0.003
MC Statistics	0.016
Fit Systematics	
$f, p^{correct}$ shape	0.011
δP_e	0.010
QCD corrections	
analysis bias	0.003
$g \rightarrow c\bar{c}$	0.001
Total	0.067

We estimated the analysis bias factor f for b events from a generator-level Monte Carlo study:

$$f = \frac{A_{q\bar{q}}^{gen} - A_{q\bar{q}+q\bar{q}g}^{analysis}}{A_{q\bar{q}}^{gen} - A_{q\bar{q}+q\bar{q}g}^{gen}}$$

We found $f = 0.89 \pm 0.10$.

From the sample of selected events we measure $A_b = 0.997 \pm 0.044$.

The error is statistical only.

5 Systematic Errors

The systematic errors for the 1997-98 SLD result can be found in Table 1. We give a brief description of the different sources.

The flavor composition error is the statistical error associated with the efficiency calibration procedure.

The analyzing power error comes mostly from calibration statistics. Also included here are the tracking efficiency uncertainties and MC statistics which impact the inter-hemisphere correlation.

The fit systematics include the shape of f and p as functions of $\cos\theta_{thr}$. These shapes are taken from the Monte Carlo and normalized by the calibrated values. The error is estimated by fitting with and without these shapes. Also included in this category is beam polarization which is needed in the fit.

The error from QCD corrections comes mainly from the uncertainty in the correction factor f . Gluon splitting is also taken into account.

6 Conclusions

We have performed a measurement of A_b using a method that takes advantage of some of the unique features of the SLC/SLD experimental program. Our preliminary result based on 250k hadronic Z^0 decays is:

$$A_c = 0.997 \pm 0.044 \pm 0.067 \quad \textbf{Preliminary}$$

This result is consistent with the SM expectation of 0.935 and other measurements at SLD and LEP. Because the systematic errors are dominated by calibration statistics this result is largely uncorrelated with other measurements.

Acknowledgements

We thank the personnel of the SLAC accelerator department and the technical staffs of our collaborating institutions for their outstanding efforts on our behalf.

*Work supported by Department of Energy contracts: DE-FG02-91ER40676 (BU), DE-FG03-91ER40618 (UCSB), DE-FG03-92ER40689 (UCSC), DE-FG03-93ER40788 (CSU), DE-FG02-91ER40672 (Colorado), DE-FG02-91ER40677 (Illinois), DE-AC03-76SF00098 (LBL), DE-FG02-92ER40715 (Massachusetts), DE-FC02-94ER40818 (MIT), DE-FG03-96ER40969 (Oregon), DE-AC03-76SF00515 (SLAC), DE-FG05-91ER40627 (Tennessee), DE-FG02-95ER40896 (Wisconsin), DE-FG02-92ER40704 (Yale); National Science Foundation grants: PHY-91-13428 (UCSC), PHY-89-21320 (Columbia), PHY-92-04239 (Cincinnati), PHY-95-10439 (Rutgers), PHY-88-19316 (Vanderbilt), PHY-92-03212 (Washington); The UK Particle Physics and Astronomy Research Council (Brunel, Oxford and RAL); The Istituto Nazionale di Fisica Nucleare of Italy (Bologna, Ferrara, Frascati, Pisa, Padova, Perugia); The Japan-US Cooperative Research Project on High Energy Physics (Nagoya, Tohoku); The Korea Research Foundation (Soongsil, 1997).

References

- [1] SLD Collab., K. Abe *et al.*, SLAC-PUB 7959, 1998.

- [2] SLD Collab., K. Abe *et al.*, Phys. Rev. Lett. **73**, 25 (1994).
- [3] SLD Collab., K. Abe *et al.*, Phys. Rev. **D53**, 1023 (1996).
- [4] M. Hildreth *et al.*, Nucl. Inst. Meth. **A367**, 111 (1995).
- [5] K. Abe *et al.*, Nucl. Inst. Meth. **A400**, 287 (1997).
- [6] D. Axen *et al.*, Nucl. Inst. Meth. **A328**, 472 (1993).
- [7] A. Benvenuti *et al.*, Nucl. Inst. Meth. **A276**, 94 (1989); **A290**, 353 (1990).
- [8] K. Abe *et al.*, Nucl. Inst. Meth. **A343**, 74 (1994).
- [9] W. Bartel *et al.*, Z. Phys. **C33**, 23 (1986).
- [10] D. Jackson, Nucl. Inst. Meth. **A388**, 247 (1997).
- [11] SLD Collab., K. Abe *et al.*, SLAC-PUB 7594, Submitted to Lepton-Photon, Hamburg, Germany, 1997.
- [12] J. B. Stav and H. A. Olsen, Phys. Rev. **D52**, 1359 (1995); Phys. Rev. **D50**, 6775 (1994).

** List of Authors

Kenji Abe,⁽²¹⁾ Koya Abe,⁽³³⁾ T. Abe,⁽²⁹⁾ I. Adam,⁽²⁹⁾ T. Akagi,⁽²⁹⁾ H. Akimoto,⁽²⁹⁾
N.J. Allen,⁽⁵⁾ W.W. Ash,⁽²⁹⁾ D. Aston,⁽²⁹⁾ K.G. Baird,⁽¹⁷⁾ C. Baltay,⁽⁴⁰⁾ H.R. Band,⁽³⁹⁾
M.B. Barakat,⁽¹⁶⁾ O. Bardon,⁽¹⁹⁾ T.L. Barklow,⁽²⁹⁾ G.L. Bashindzhagyan,⁽²⁰⁾
J.M. Bauer,⁽¹⁸⁾ G. Bellodi,⁽²³⁾ A.C. Benvenuti,⁽³⁾ G.M. Bilei,⁽²⁵⁾ D. Bisello,⁽²⁴⁾
G. Blaylock,⁽¹⁷⁾ J.R. Bogart,⁽²⁹⁾ G.R. Bower,⁽²⁹⁾ J.E. Brau,⁽²²⁾ M. Breidenbach,⁽²⁹⁾
W.M. Bugg,⁽³²⁾ D. Burke,⁽²⁹⁾ T.H. Burnett,⁽³⁸⁾ P.N. Burrows,⁽²³⁾ R.M. Byrne,⁽¹⁹⁾
A. Calcaterra,⁽¹²⁾ D. Calloway,⁽²⁹⁾ B. Camanzi,⁽¹¹⁾ M. Carpinelli,⁽²⁶⁾ R. Cassell,⁽²⁹⁾
R. Castaldi,⁽²⁶⁾ A. Castro,⁽²⁴⁾ M. Cavalli-Sforza,⁽³⁵⁾ A. Chou,⁽²⁹⁾ E. Church,⁽³⁸⁾
H.O. Cohn,⁽³²⁾ J.A. Coller,⁽⁶⁾ M.R. Convery,⁽²⁹⁾ V. Cook,⁽³⁸⁾ R.F. Cowan,⁽¹⁹⁾
D.G. Coyne,⁽³⁵⁾ G. Crawford,⁽²⁹⁾ C.J.S. Damerell,⁽²⁷⁾ M.N. Danielson,⁽⁸⁾ M. Daoudi,⁽²⁹⁾
N. de Groot,⁽⁴⁾ R. Dell'Orso,⁽²⁵⁾ P.J. Dervan,⁽⁵⁾ R. de Sangro,⁽¹²⁾ M. Dima,⁽¹⁰⁾
D.N. Dong,⁽¹⁹⁾ M. Doser,⁽²⁹⁾ R. Dubois,⁽²⁹⁾ B.I. Eisenstein,⁽¹³⁾ I. Erofeeva,⁽²⁰⁾
V. Eschenburg,⁽¹⁸⁾ E. Etzion,⁽³⁹⁾ S. Fahey,⁽⁸⁾ D. Falciari,⁽¹²⁾ C. Fan,⁽⁸⁾ J.P. Fernandez,⁽³⁵⁾
M.J. Fero,⁽¹⁹⁾ K. Flood,⁽¹⁷⁾ R. Frey,⁽²²⁾ J. Gifford,⁽³⁶⁾ T. Gillman,⁽²⁷⁾ G. Gladding,⁽¹³⁾
S. Gonzalez,⁽¹⁹⁾ E.R. Goodman,⁽⁸⁾ E.L. Hart,⁽³²⁾ J.L. Harton,⁽¹⁰⁾ K. Hasuko,⁽³³⁾
S.J. Hedges,⁽⁶⁾ S.S. Hertzbach,⁽¹⁷⁾ M.D. Hildreth,⁽²⁹⁾ J. Huber,⁽²²⁾ M.E. Huffer,⁽²⁹⁾
E.W. Hughes,⁽²⁹⁾ X. Huynh,⁽²⁹⁾ H. Hwang,⁽²²⁾ M. Iwasaki,⁽²²⁾ D.J. Jackson,⁽²⁷⁾
P. Jacques,⁽²⁸⁾ J.A. Jaros,⁽²⁹⁾ Z.Y. Jiang,⁽²⁹⁾ A.S. Johnson,⁽²⁹⁾ J.R. Johnson,⁽³⁹⁾
R.A. Johnson,⁽⁷⁾ T. Junk,⁽²⁹⁾ R. Kajikawa,⁽²¹⁾ M. Kalelkar,⁽²⁸⁾ Y. Kamyshev,⁽³²⁾
H.J. Kang,⁽²⁸⁾ I. Karliner,⁽¹³⁾ H. Kawahara,⁽²⁹⁾ Y.D. Kim,⁽³⁰⁾ M.E. King,⁽²⁹⁾ R. King,⁽²⁹⁾
R.R. Kofler,⁽¹⁷⁾ N.M. Krishna,⁽⁸⁾ R.S. Kroeger,⁽¹⁸⁾ M. Langston,⁽²²⁾ A. Lath,⁽¹⁹⁾
D.W.G. Leith,⁽²⁹⁾ V. Lia,⁽¹⁹⁾ C. Lin,⁽¹⁷⁾ M.X. Liu,⁽⁴⁰⁾ X. Liu,⁽³⁵⁾ M. Loreti,⁽²⁴⁾ A. Lu,⁽³⁴⁾

H.L. Lynch,⁽²⁹⁾ J. Ma,⁽³⁸⁾ M. Mahjouri,⁽¹⁹⁾ G. Mancinelli,⁽²⁸⁾ S. Manly,⁽⁴⁰⁾
 G. Mantovani,⁽²⁵⁾ T.W. Markiewicz,⁽²⁹⁾ T. Maruyama,⁽²⁹⁾ H. Masuda,⁽²⁹⁾ E. Mazzucato,⁽¹¹⁾
 A.K. McKemey,⁽⁵⁾ B.T. Meadows,⁽⁷⁾ G. Menegatti,⁽¹¹⁾ R. Messner,⁽²⁹⁾ P.M. Mockett,⁽³⁸⁾
 K.C. Moffeit,⁽²⁹⁾ T.B. Moore,⁽⁴⁰⁾ M. Morii,⁽²⁹⁾ D. Muller,⁽²⁹⁾ V. Murzin,⁽²⁰⁾ T. Nagamine,⁽³³⁾
 S. Narita,⁽³³⁾ U. Nauenberg,⁽⁸⁾ H. Neal,⁽²⁹⁾ M. Nussbaum,⁽⁷⁾ N. Oishi,⁽²¹⁾
 D. Onoprienko,⁽³²⁾ L.S. Osborne,⁽¹⁹⁾ R.S. Panvini,⁽³⁷⁾ C.H. Park,⁽³¹⁾ T.J. Pavel,⁽²⁹⁾
 I. Peruzzi,⁽¹²⁾ M. Piccolo,⁽¹²⁾ L. Piemontese,⁽¹¹⁾ K.T. Pitts,⁽²²⁾ R.J. Plano,⁽²⁸⁾
 R. Prepost,⁽³⁹⁾ C.Y. Prescott,⁽²⁹⁾ G.D. Punkar,⁽²⁹⁾ J. Quigley,⁽¹⁹⁾ B.N. Ratcliff,⁽²⁹⁾
 T.W. Reeves,⁽³⁷⁾ J. Reidy,⁽¹⁸⁾ P.L. Reinertsen,⁽³⁵⁾ P.E. Rensing,⁽²⁹⁾ L.S. Rochester,⁽²⁹⁾
 P.C. Rowson,⁽⁹⁾ J.J. Russell,⁽²⁹⁾ O.H. Saxton,⁽²⁹⁾ T. Schalk,⁽³⁵⁾ R.H. Schindler,⁽²⁹⁾
 B.A. Schumm,⁽³⁵⁾ J. Schwiening,⁽²⁹⁾ S. Sen,⁽⁴⁰⁾ V.V. Serbo,⁽²⁹⁾ M.H. Shaevitz,⁽⁹⁾
 J.T. Shank,⁽⁶⁾ G. Shapiro,⁽¹⁵⁾ D.J. Sherden,⁽²⁹⁾ K.D. Shmakov,⁽³²⁾ C. Simopoulos,⁽²⁹⁾
 N.B. Sinev,⁽²²⁾ S.R. Smith,⁽²⁹⁾ M.B. Smy,⁽¹⁰⁾ J.A. Snyder,⁽⁴⁰⁾ H. Staengle,⁽¹⁰⁾ A. Stahl,⁽²⁹⁾
 P. Stamer,⁽²⁸⁾ H. Steiner,⁽¹⁵⁾ R. Steiner,⁽¹⁾ M.G. Strauss,⁽¹⁷⁾ D. Su,⁽²⁹⁾ F. Suekane,⁽³³⁾
 A. Sugiyama,⁽²¹⁾ S. Suzuki,⁽²¹⁾ M. Swartz,⁽¹⁴⁾ A. Szumilo,⁽³⁸⁾ T. Takahashi,⁽²⁹⁾
 F.E. Taylor,⁽¹⁹⁾ J. Thom,⁽²⁹⁾ E. Torrence,⁽¹⁹⁾ N.K. Toumbas,⁽²⁹⁾ T. Usher,⁽²⁹⁾
 C. Vannini,⁽²⁶⁾ J. Va'vra,⁽²⁹⁾ E. Vella,⁽²⁹⁾ J.P. Venuti,⁽³⁷⁾ R. Verdier,⁽¹⁹⁾ P.G. Verdini,⁽²⁶⁾
 D.L. Wagner,⁽⁸⁾ S.R. Wagner,⁽²⁹⁾ A.P. Waite,⁽²⁹⁾ S. Walston,⁽²²⁾ S.J. Watts,⁽⁵⁾
 A.W. Weidemann,⁽³²⁾ E. R. Weiss,⁽³⁸⁾ J.S. Whitaker,⁽⁶⁾ S.L. White,⁽³²⁾ F.J. Wickens,⁽²⁷⁾
 B. Williams,⁽⁸⁾ D.C. Williams,⁽¹⁹⁾ S.H. Williams,⁽²⁹⁾ S. Willocq,⁽¹⁷⁾ R.J. Wilson,⁽¹⁰⁾
 W.J. Wisniewski,⁽²⁹⁾ J. L. Wittlin,⁽¹⁷⁾ M. Woods,⁽²⁹⁾ G.B. Word,⁽³⁷⁾ T.R. Wright,⁽³⁹⁾
 J. Wyss,⁽²⁴⁾ R.K. Yamamoto,⁽¹⁹⁾ J.M. Yamartino,⁽¹⁹⁾ X. Yang,⁽²²⁾ J. Yashima,⁽³³⁾
 S.J. Yellin,⁽³⁴⁾ C.C. Young,⁽²⁹⁾ H. Yuta,⁽²⁾ G. Zapalac,⁽³⁹⁾ R.W. Zdarko,⁽²⁹⁾ J. Zhou.⁽²²⁾

(The SLD Collaboration)

- ⁽¹⁾ *Adelphi University, Garden City, New York 11530,*
- ⁽²⁾ *Aomori University, Aomori, 030 Japan,*
- ⁽³⁾ *INFN Sezione di Bologna, I-40126, Bologna, Italy,*
- ⁽⁴⁾ *University of Bristol, Bristol, U.K.,*
- ⁽⁵⁾ *Brunel University, Uxbridge, Middlesex, UB8 3PH United Kingdom,*
- ⁽⁶⁾ *Boston University, Boston, Massachusetts 02215,*
- ⁽⁷⁾ *University of Cincinnati, Cincinnati, Ohio 45221,*
- ⁽⁸⁾ *University of Colorado, Boulder, Colorado 80309,*
- ⁽⁹⁾ *Columbia University, New York, New York 10533,*
- ⁽¹⁰⁾ *Colorado State University, Ft. Collins, Colorado 80523,*
- ⁽¹¹⁾ *INFN Sezione di Ferrara and Università di Ferrara, I-44100 Ferrara, Italy,*
- ⁽¹²⁾ *INFN Lab. Nazionali di Frascati, I-00044 Frascati, Italy,*
- ⁽¹³⁾ *University of Illinois, Urbana, Illinois 61801,*
- ⁽¹⁴⁾ *Johns Hopkins University, Baltimore, Maryland 21218-2686,*
- ⁽¹⁵⁾ *Lawrence Berkeley Laboratory, University of California, Berkeley, California 94720,*
- ⁽¹⁶⁾ *Louisiana Technical University, Ruston, Louisiana 71272,*
- ⁽¹⁷⁾ *University of Massachusetts, Amherst, Massachusetts 01003,*
- ⁽¹⁸⁾ *University of Mississippi, University, Mississippi 38677,*
- ⁽¹⁹⁾ *Massachusetts Institute of Technology, Cambridge, Massachusetts 02139,*
- ⁽²⁰⁾ *Institute of Nuclear Physics, Moscow State University, 119899, Moscow Russia,*
- ⁽²¹⁾ *Nagoya University, Chikusa-ku, Nagoya, 464 Japan,*

- ⁽²²⁾ *University of Oregon, Eugene, Oregon 97403,*
- ⁽²³⁾ *Oxford University, Oxford, OX1 3RH, United Kingdom,*
- ⁽²⁴⁾ *INFN Sezione di Padova and Universita di Padova I-35100, Padova, Italy,*
- ⁽²⁵⁾ *INFN Sezione di Perugia and Universita di Perugia, I-06100 Perugia, Italy,*
- ⁽²⁶⁾ *INFN Sezione di Pisa and Universita di Pisa, I-56010 Pisa, Italy,*
- ⁽²⁷⁾ *Rutherford Appleton Laboratory, Chilton, Didcot, Oxon OX11 0QX United Kingdom,*
- ⁽²⁸⁾ *Rutgers University, Piscataway, New Jersey 08855,*
- ⁽²⁹⁾ *Stanford Linear Accelerator Center, Stanford University, Stanford, California 94309,*
- ⁽³⁰⁾ *Sogang University, Seoul, Korea,*
- ⁽³¹⁾ *Soongsil University, Seoul, Korea 156-743,*
- ⁽³²⁾ *University of Tennessee, Knoxville, Tennessee 37996,*
- ⁽³³⁾ *Tohoku University, Sendai 980, Japan,*
- ⁽³⁴⁾ *University of California at Santa Barbara, Santa Barbara, California 93106,*
- ⁽³⁵⁾ *University of California at Santa Cruz, Santa Cruz, California 95064,*
- ⁽³⁶⁾ *University of Victoria, Victoria, British Columbia, Canada V8W 3P6,*
- ⁽³⁷⁾ *Vanderbilt University, Nashville, Tennessee 37235,*
- ⁽³⁸⁾ *University of Washington, Seattle, Washington 98105,*
- ⁽³⁹⁾ *University of Wisconsin, Madison, Wisconsin 53706,*
- ⁽⁴⁰⁾ *Yale University, New Haven, Connecticut 06511.*